

Domain Decomposition Solvers for Nonlinear Multiharmonic Finite Element Equations

D. Copeland, U. Langer

RICAM-Report 2009-20

DOMAIN DECOMPOSITION SOLVERS FOR NONLINEAR MULTIHARMONIC FINITE ELEMENT EQUATIONS

DYLAN M. COPELAND* AND ULRICH LANGER†

Abstract. In many practical applications, for instance, in computational electromagnetics, the excitation is time-harmonic. Switching from the time domain to the frequency domain allows us to replace the expensive time-integration procedure by the solution of a simple elliptic equation for the amplitude. This is true for linear problems, but not for nonlinear problems. However, due to the periodicity of the solution, we can expand the solution in a Fourier series. Truncating this Fourier series and approximating the Fourier coefficients by finite elements, we arrive at a large-scale coupled nonlinear system for determining the finite element approximation to the Fourier coefficients. The construction of fast solvers for such systems is very crucial for the efficiency of this multiharmonic approach. In this paper we look at nonlinear, time-harmonic potential problems as simple model problems. We construct and analyze almost optimal solvers for the Jacobi systems arising from the Newton linearization of the large-scale coupled nonlinear system that one has to solve instead of performing the expensive time-integration procedure.

1. Introduction. In many practical applications, the excitation is time-harmonic with some frequency ω . In order to avoid a time-consuming time-integration method, we can switch from the time domain to the frequency domain, where we only have to solve some elliptic boundary value problem, for instance, by the use of the finite element method (FEM). This is true for linear problems, but not for nonlinear problems. Due to the nonlinearity we cannot assume that the solution $u(x, t)$ only depends on the harmonics of the excitation as in the linear case where we make use of the ansatz $u(x, t) = \hat{u}(x) \exp(i\omega t)$ with the amplitude $\hat{u}(x)$. However, due to the periodicity of the solution, we can expand the solution in a Fourier series. Truncating this Fourier series and approximating the Fourier coefficients by finite elements, we arrive at a large-scale coupled nonlinear system for determining the finite element approximations to finitely many Fourier coefficients. In the literature, this approach is called multiharmonic FEM or harmonic-balanced FEM, and has been used by many engineers in different applications, see, e.g., [1], [6], [7], [14], [22], and the references therein.

In [2], F. Bachinger, U. Langer and J. Schöberl provide the first rigorous numerical analysis for the eddy current problem. The practical aspects of the multiharmonic approach, including the construction of a fast multigrid preconditioned QMR solver for the Jacobi system arising in every Newton step and the implementation in an adaptive multilevel setting, are discussed in [3] by the same authors. There was no rigorous analysis of the multigrid preconditioned QMR solver, but the numerical results presented in this paper for academic and more practical problems indicated the efficiency of this solver.

In this paper, instead of the eddy current problem, we consider as our model problem the following nonlinear, parabolic, scalar potential equation, with a homogeneous Dirichlet boundary condition and an inhomogeneous initial condition:

$$(1.1) \quad \begin{cases} \alpha \frac{\partial u}{\partial t} - \nabla \cdot (\nu(|\nabla u|) \nabla u) = f & \text{in } \Omega \times (0, T], \\ u(\mathbf{x}, 0) = u_0(\mathbf{x}) & \text{in } \bar{\Omega}, \\ u(\mathbf{x}, t) = 0 & \text{on } \partial\Omega \times [0, T]. \end{cases}$$

*The Institute for Applied Mathematics and Computational Science, Texas A&M University, College Station, USA, e-mail: copeland@math.tamu.edu

†Institute of Computational Mathematics, Johannes Kepler University, Linz, Austria, e-mail: ulanger@numa.uni-linz.ac.at

Here, the coefficient $\nu(|\nabla u|)$ plays the same role as the reluctivity in the eddy current problem discussed in [2] and [3], and the right-hand side $f(x, t)$ is given by a harmonic excitation with the frequency ω . We assume that $\Omega \subset \mathbb{R}^3$ is a bounded Lipschitz domain, α is a given uniformly positive function in $L_\infty(\Omega)$, and $\nu : \mathbb{R}_0^+ \rightarrow \mathbb{R}^+$ is a continuously differentiable function satisfying the properties

$$(1.2) \quad 0 < \nu_{\min} \leq \nu(s) \leq \nu_{\max} \quad \text{for } s \geq 0,$$

$$(1.3) \quad s \mapsto s\nu(s) \quad \text{is Lipschitz and strongly monotone for } s \geq 0.$$

These conditions for ν are naturally satisfied in applications modeled with the **B-H** curve (see [15, 16]). Monotonicity is necessary for our theory, which uses monotonicity to ensure unique solvability.

We mention that a two-dimensional eddy current problem can be reduced to a nonlinear parabolic problem like (1.1), where α can vanish in non-conducting materials like air. In [2], the so-called conductivity regularization was used to treat this problem. Applying the multiharmonic approach to (1.1), we finally arrive at a large-scale nonlinear system of algebraic equations for determining the finite element approximations to Fourier coefficients, cf. [3]. This nonlinear system can be solved by the Newton method. The efficiency of the Newton method mainly depends on the availability of some fast solver for the Jacobi system arising in each step of the Newton iteration. The construction and the analysis of an almost optimal preconditioner for the Jacobi matrices is the main topic of this paper. The preconditioner is based on a non-overlapping domain decomposition and is used in a GMRES iteration. The construction and analysis are heavily based on results obtained in [21], [3], [9] and [10].

The rest of the paper is organized as follows. In Section 2, we apply the multiharmonic approach to the nonlinear parabolic problem (1.1). Here we use the same real-valued setting as in [2] and [3]. Section 3 is devoted to the linear case where only the excitation frequency is involved. The linear case provides a foundation for subsequently developing a similar solver for the nonlinear case. The resulting system of finite element equations has a nonsymmetric but positive definite system matrix, which can be solved efficiently by a preconditioned GMRES method. In Section 4, we construct a preconditioner that is based on a non-overlapping domain decomposition and analyze the convergence rate of the corresponding preconditioned GMRES method. This solver is then used for solving the linear systems arising at each step of Newton's method. This complete solution procedure for nonlinear finite element equations is discussed in Section 5. In Section 6, we present our numerical results confirming the rate estimates given in Section 4. Section 7 draws some conclusions.

2. The Multiharmonic Approach. Assuming that the solution u to (1.1) is periodic in time, with frequency ω , we have the Fourier series representation

$$u(\mathbf{x}, t) = \sum_{k=0}^{\infty} u_k^c(\mathbf{x}) \cos(k\omega t) + u_k^s(\mathbf{x}) \sin(k\omega t),$$

where the Fourier coefficients are given by

$$u_k^c(\mathbf{x}) = \frac{2}{T} \int_0^T u(\mathbf{x}, t) \cos(k\omega t) dt, \quad u_k^s(\mathbf{x}) = \frac{2}{T} \int_0^T u(\mathbf{x}, t) \sin(k\omega t) dt.$$

Here, the period is $T = 2\pi/\omega$. Similarly, the potential

$$\Psi[u](\mathbf{x}, t) := \nu(|\nabla u|) \nabla u(\mathbf{x}, t)$$

As a variational formulation, we seek the vector-function $\mathbf{u} = (u_1^c, u_1^s, \dots, u_N^c, u_N^s)^T$ of the Fourier coefficients in $H_0^1(\Omega)^{2N}$ satisfying

$$(2.4) \quad (L^{(N)}\mathbf{u}, \mathbf{v}) + \omega(\alpha D_N \mathbf{u}, \mathbf{v}) = (\mathbf{f}, \mathbf{v}) \quad \text{for all } \mathbf{v} \text{ in } H_0^1(\Omega)^{2N},$$

where

$$(L^{(N)}\mathbf{u}, \mathbf{v}) := \int_{\Omega} \Psi(\mathbf{u}) \cdot \nabla \mathbf{v} \, d\mathbf{x} = \int_{\Omega} \nu(|\nabla \tilde{u}|) \nabla \mathbf{u} \cdot \nabla \mathbf{v} \, d\mathbf{x}$$

for all \mathbf{u}, \mathbf{v} in $H_0^1(\Omega)^{2N}$. Here, the gradient operator $\nabla : H_0^1(\Omega)^{2N} \rightarrow ((L_2(\Omega))^3)^{2N}$ is applied entry-wise. The unique solvability of this variational formulation follows simply from the strong monotonicity and the Lipschitz-continuity of the operator $L^{(N)}$ and the nonlinear version of the Lax-Milgram lemma (cf. [15, 23]).

REMARK 2. *It is shown in [2, Theorem 13] that the convergence of the multi-harmonic approximation (2.1) is generally of order $O(N^{-1})$. However, in the case of excitation by one harmonic, numerical experiments have shown exponential convergence in the number of harmonics N . In such applications, very few (typically less than 10) harmonics are needed in order to obtain an accurate solution (cf. [3]).*

3. The Linear Case. In the case that ν is independent of $|\nabla \tilde{u}|$ and the right-hand-side f is of the form

$$f(\mathbf{x}, t) = f^c(\mathbf{x}) \cos(\omega t) + f^s(\mathbf{x}) \sin(\omega t),$$

the solution u depends only on the frequency ω and can also be expressed as

$$u(\mathbf{x}, t) = u^c(\mathbf{x}) \cos(\omega t) + u^s(\mathbf{x}) \sin(\omega t).$$

Consider the bilinear form

$$(3.1) \quad a(\mathbf{u}, \mathbf{v}) := \left(\begin{pmatrix} L & \omega \alpha I \\ -\omega \alpha I & L \end{pmatrix} \mathbf{u}, \mathbf{v} \right) = (L^{(1)}\mathbf{u}, \mathbf{v}) + \omega(\alpha D_1 \mathbf{u}, \mathbf{v})$$

defined for \mathbf{u}, \mathbf{v} in $H_0^1(\Omega)^2$, where

$$(L\phi, \psi) := \int_{\Omega} \nu \nabla \phi \cdot \nabla \psi \, d\mathbf{x}, \quad \text{for all } \phi, \psi \text{ in } H_0^1(\Omega),$$

is the Dirichlet form. Note that the bilinear form $a(\cdot, \cdot)$ is the sum of a symmetric, positive definite bilinear form $(L^{(1)}\cdot, \cdot)$ and a skew-symmetric bilinear form $\omega(\alpha D_1 \cdot, \cdot)$. Thus the symmetric part is positive definite, as

$$(3.2) \quad a(\mathbf{u}, \mathbf{u}) = (L^{(1)}\mathbf{u}, \mathbf{u}) \geq C \|\mathbf{u}\|_{H^1(\Omega)^2}^2, \quad \text{for all } \mathbf{u} \text{ in } H_0^1(\Omega)^2.$$

The variational problem for the linear case is to find $\mathbf{u} = (u^c, u^s)$ in $H_0^1(\Omega)^2$ satisfying

$$(3.3) \quad a(\mathbf{u}, \mathbf{v}) = (\mathbf{f}, \mathbf{v}) \quad \text{for all } \mathbf{v} \text{ in } H_0^1(\Omega)^2,$$

where $\mathbf{f} = (f^c, f^s)$ is given in $L_2(\Omega)^2$. The variational problem (3.3) is nothing but the real variational reformulation of the complex time-domain problem

$$(3.4) \quad -\nabla \cdot (\nu \nabla \hat{u}) + i\omega \alpha \hat{u} = \hat{f} \text{ in } \Omega \quad \text{and} \quad \hat{u} = 0 \text{ on } \partial\Omega,$$

following from the linear version of the parabolic initial-boundary value problem via the ansatz $u(x, t) = \hat{u}(x) \exp(i\omega t)$, assuming a harmonic excitation of the form $f(x, t) = \hat{f}(x) \exp(i\omega t)$ with the complex amplitudes $\hat{f}(x) = f^c(x) - if^s(x)$ and $\hat{u}(x) = u^c(x) - iu^s(x)$.

For discretization, the space $H_0^1(\Omega)$ is approximated by the finite element space S_1^h of continuous piecewise linear functions, with the standard nodal basis $\{\phi_j\}_{j=1}^{l_h}$. Approximating $H_0^1(\Omega)^2$ by the finite dimensional space $\mathbf{S}_h^1 := \left(\text{span}\{\phi_j\}_{j=1}^{l_h}\right)^2$, we discretize the variational problem (3.3) by the nonsymmetric system of linear equations

$$(3.5) \quad (A + M)\xi = f,$$

defined by

$$A_{ij} = (L^{(1)}\phi_i, \phi_j), \quad M_{ij} = \omega(\alpha D_1\phi_i, \phi_j), \quad f_i = (f, \phi_i),$$

where $\{\phi_j\}_{j=1}^{2l_h}$ is the standard nodal basis for \mathbf{S}_h^1 , and $\xi = [\xi_j]_{j=1}^{2l_h}$ is the vector of coefficients in \mathbb{R}^{2l_h} . Thus $\mathbf{u}_h = \sum_{j=1}^{2l_h} \xi_j \phi_j$ is the finite element approximation to \mathbf{u} . The nonsymmetric system (3.5) can be solved by an iterative method such as GMRES or QMR, with a preconditioner as proposed in the next section.

4. Preconditioning via Domain Decomposition. Following [21], we propose a preconditioner for (3.5) of the form

$$(4.1) \quad B_{A+M} = A_0^{-1}Q_0 + \beta B,$$

where B is a symmetric positive definite preconditioner for A , β is a positive scaling constant, Q_0 is the L_2 -orthogonal projector from \mathbf{S}_h^1 onto some coarse subspace \mathbf{V}_0 , and A_0 is the restriction of $A + M$ to \mathbf{V}_0 . To be precise, $Q_0 : L_2(\Omega)^2 \rightarrow \mathbf{V}_0$ and $A_0 : \mathbf{V}_0 \rightarrow \mathbf{V}_0$ are defined by

$$(Q_0\mathbf{u}, \mathbf{v}_0) = (\mathbf{u}, \mathbf{v}_0) \text{ for all } \mathbf{u} \text{ in } L_2(\Omega)^2, \mathbf{v}_0 \text{ in } \mathbf{V}_0,$$

and

$$(A_0\mathbf{u}_0, \mathbf{v}_0) = ((A + M)\mathbf{u}_0, \mathbf{v}_0) \text{ for all } \mathbf{u}_0, \mathbf{v}_0 \text{ in } \mathbf{V}_0,$$

respectively. Let $\bar{\Omega} = \cup_{j=1}^p \bar{\Omega}_j$ be a non-overlapping domain decomposition, and let $\Gamma := \cup_{j=1}^p \partial\Omega_j \setminus \partial\Omega$ denote the interface. For the construction of a simple coarse space \mathbf{V}_0 , we assume that the subdomains Ω_j are elements of a conforming tetrahedral mesh of size H . Then \mathbf{V}_0 is taken to be \mathbf{S}_H^1 , the space of continuous piecewise linear functions with respect to the subdomains Ω_j .

A wire-basket-based domain decomposition method gives an effective preconditioner B for the symmetric positive definite matrix A , with a condition number estimate independent of jumps in the coefficient. The method we now describe is Algorithm 5.10 of [20] (see also [4]). The action of B on a vector \mathbf{v}_h in \mathbf{S}_h^1 is defined as follows, by considering $\mathbf{w}_h := A^{-1}\mathbf{v}_h$ in \mathbf{S}_h^1 . We partition the degrees of freedom \mathbf{w}_h into those on the interface, \mathbf{w}_B , and those in the interiors of the subdomains, \mathbf{w}_I . Similarly, the matrix A is partitioned as

$$A = \begin{pmatrix} A_{II} & A_{IB} \\ A_{IB}^T & A_{BB} \end{pmatrix}.$$

Reducing the system $A\mathbf{w}_h = \mathbf{v}_h$ to the degrees of freedom on the interface Γ via local Schur complements yields the system

$$S\mathbf{w}_B = \sum_{j=1}^p (A_{BB}^{(j)} - A_{IB}^{(j)T} A_{II}^{(j)-1} A_{IB}^{(j)}) \mathbf{w}_B^{(j)} = \sum_{j=1}^p \mathbf{v}_B^{(j)} - A_{IB}^{(j)T} A_{II}^{(j)-1} \mathbf{v}_I^{(j)},$$

where the superscript (j) denotes the restriction of a matrix or vector to the subdomain $\bar{\Omega}_j$.

The preconditioner B , defined by

$$B := \begin{pmatrix} I & -E_{IB} \\ 0 & I \end{pmatrix} \begin{pmatrix} B_I^{-1} & 0 \\ 0 & B_S^{-1} \end{pmatrix} \begin{pmatrix} I & 0 \\ -E_{IB}^T & I \end{pmatrix},$$

approximates A^{-1} in view of the factorization

$$A^{-1} := \begin{pmatrix} I & -A_I^{-1} A_{IB} \\ 0 & I \end{pmatrix} \begin{pmatrix} A_I^{-1} & 0 \\ 0 & S^{-1} \end{pmatrix} \begin{pmatrix} I & 0 \\ -A_{IB}^T A_I^{-1} & I \end{pmatrix},$$

where E_{IB} denotes an extension operator from the interface to the interior of the subdomains, and B_I^{-1} and B_S^{-1} are preconditioners for A_{II} and S , respectively, [11], see also [9, 10, 8, 12]. The inverse A_I^{-1} can be replaced by a multigrid preconditioner T_L for the diagonal blocks of A_{II} , which are Galerkin discretizations of the operator L . The preconditioner

$$B_I^{-1} := \begin{pmatrix} T_L & 0 \\ 0 & T_L \end{pmatrix}$$

is spectrally equivalent to A_{II}^{-1} , with constants independent of the mesh parameters (see, e.g., [13]). The choice $E_{IB} = B_I^{-1} A_{IB}$, with an optimal multigrid preconditioner B_I^{-1} for A_{II} , does not lead to an optimal extension operator [10]. There is an additional logarithmic factor. However, G. Haase and S.V. Nepomnyaschikh proposed multilevel extension operators which avoid additional logarithmic factors [12].

The wire-basket-based additive Schwarz preconditioner B_S^{-1} is defined as follows. First, consider the representation

$$S = \begin{pmatrix} I & 0 \\ -T & I \end{pmatrix} \begin{pmatrix} S_{FF} & S_{FW} \\ S_{FW}^T & S_{WW} \end{pmatrix} \begin{pmatrix} I & -T^T \\ 0 & I \end{pmatrix},$$

where the degrees of freedom are partitioned by faces (F) and the wire basket (W), and T^T maps the average of the nodal values on the boundary of each face to the nodes in the face. Dropping the coupling between vertices on the faces and the wire basket results in the approximate inverse

$$(4.2) \quad \begin{pmatrix} I & T^T \\ 0 & I \end{pmatrix} \begin{pmatrix} S_{FF}^{-1} & 0 \\ 0 & S_{WW}^{-1} \end{pmatrix} \begin{pmatrix} I & -T^T \\ 0 & I \end{pmatrix}.$$

The restriction S_{WW} of S to the nodal functions on the wire basket is replaced by the bilinear form $b_0^W(\cdot, \cdot)$ on the coarse space $\mathbf{S}_h^W := (\text{range } I_h^W)^2$, where I_h^W is defined on S_h^1 by

$$I_h^W u_h = \sum_{\mathbf{x}_k \in W_h} u_h(\mathbf{x}_k) \psi_k + \sum_k \bar{u}_{h, \partial F^k} \theta_{F^k}.$$

Here, ψ_k is the discrete harmonic extension of the nodal basis function associated with the vertex \mathbf{x}_k , $\bar{u}_{h,\partial F^k}$ is the average of the nodal values of u_h on ∂F^k , and θ_{F^k} is the function in S_h^1 equal to 1 on $F^k = \partial\Omega_i \cap \partial\Omega_j$, vanishing on $\partial\Omega_i \cap \partial\Omega_j \setminus F^k$, and discrete harmonic in Ω_i and Ω_j . The quadratic form $b_0^W(\cdot, \cdot)$ is defined by

$$b_0^W(\mathbf{u}_h, \mathbf{u}_h) = (1 + \log(H/h))h \sum_i \nu_i \min_{\gamma_i} \|\mathbf{u}_h - \gamma_i \mathbf{1}^{(i)}\|_{l^2(W^i)}^2,$$

where $\mathbf{1}$ is the vector with all entries equal to one (cf. [19]). Now B_S^{-1} is defined by replacing S_{WW} in (4.2) by the matrix given by $b_0^W(\cdot, \cdot)$ on \mathbf{S}_h^W . The condition number estimate

$$(4.3) \quad \kappa(B_S^{-1}S) \leq C(1 + \log(H/h))^2$$

is proven in [4, Theorem 6.4]. This estimate and the results from [9, 10, 8, 11, 12] give the bounds

$$(4.4) \quad C(1 + \log(H/h))^{-2} \leq \lambda_{\min}(BA) \quad \text{and} \quad \lambda_{\max}(BA) \leq C$$

for the extreme eigenvalues of BA .

The construction of the preconditioner B_{A+M} is now complete, except for a coarse solver to compute the action of A_0^{-1} . The nonsymmetric coarse space operator A_0 can be preconditioned with a multigrid method for a symmetric system, as done in [3]. Consider the expression

$$A_0 = \begin{pmatrix} A_0^L & A_0^{\omega\alpha} \\ -A_0^{\omega\alpha} & A_0^L \end{pmatrix},$$

where the submatrices A_0^L and $A_0^{\omega\alpha}$ are the Galerkin discretizations of the operators L and $\omega\alpha I$ (cf. (3.1)), respectively. A good preconditioner for A_0 is

$$\tilde{B}_0^{-1} := \frac{1}{2} \begin{pmatrix} (A_0^L + A_0^{\omega\alpha})^{-1} & 0 \\ 0 & (A_0^L + A_0^{\omega\alpha})^{-1} \end{pmatrix} \begin{pmatrix} I & I \\ I & -I \end{pmatrix}.$$

By [3, Lemma 1], we have the condition number estimate

$$\kappa(\tilde{B}_0^{-1}(A_0^L + A_0^{\omega\alpha})) \leq 2.$$

The inverse $(A_0^L + A_0^{\omega\alpha})^{-1}$ can be approximated by a multigrid cycle T_L for $A_0^L + A_0^{\omega\alpha}$, yielding the preconditioner

$$(4.5) \quad B_0^{-1} := \frac{1}{2} \begin{pmatrix} T_L & 0 \\ 0 & T_L \end{pmatrix} \begin{pmatrix} I & I \\ I & -I \end{pmatrix}.$$

This preconditioner performs well in practice, but we do not use it for solving the problem (3.5) on the fine level due to the lack of convergence theory. Instead, we propose the preconditioner B_{A+M} for which we can provide convergence rate estimates.

Now we are in position to prove our main result, namely Theorem 1, which gives a convergence rate estimate for the GMRES method applied to (3.5) with the preconditioner B_{A+M} . The convergence rate is given in the norm $\|\cdot\|_A$ induced by the inner product $(\cdot, \cdot)_A$, defined by $(\mathbf{v}_h, \mathbf{w}_h)_A := (A\mathbf{v}_h, \mathbf{w}_h)$ for \mathbf{v}_h and \mathbf{w}_h in \mathbf{S}_h^1 . First, we prove the following lemma.

LEMMA 1. *Assume that the solution of the boundary value problem adjoint to (3.3) satisfies the regularity estimate $\|\mathbf{u}\|_{H^{1+s}(\Omega)^2} \leq C\|\mathbf{f}\|_{L_2(\Omega)^2}$ for any given right-hand side $\mathbf{f} \in L_2(\Omega)^2$ with some $s \in (0, 1]$, and H is sufficiently small, specifically $H^s < C(1 + \log(H/h))^{-2}$. Then for all \mathbf{u}_h in \mathbf{S}_h^1 , we have*

$$(4.6) \quad \|B_{A+M}(A+M)\mathbf{u}_h\|_A \leq C(1 + (1 + \log(H/h))^{-2})\|\mathbf{u}_h\|_A,$$

$$(4.7) \quad (B_{A+M}(A+M)\mathbf{u}_h, \mathbf{u}_h)_A \geq C(1 + \log(H/h))^{-4}(\mathbf{u}_h, \mathbf{u}_h)_A.$$

The constants here depend only on α , ν , and ω .

Proof. The result with generic constants is given by [21, Theorem 1]. To prove (4.6) and (4.7), we need only determine the dependence of the constants on the mesh and subdomain parameters h and H . Consider constants C_1 and C_2 such that

$$(4.8) \quad \|\mathbf{u}_h\| \leq C_1\|\mathbf{u}_h\|_A \quad \text{for all } \mathbf{u}_h \text{ in } \mathbf{S}_h^1,$$

and

$$(4.9) \quad (M\mathbf{u}_h, \mathbf{v}_h) \leq C_2\|\mathbf{u}_h\|\|\mathbf{v}_h\|_A \quad \text{for all } \mathbf{u}_h, \mathbf{v}_h \text{ in } \mathbf{S}_h^1.$$

Clearly, (4.8) holds with $C_1 = C_P\nu_{min}^{-1}$, where C_P is given by the Poincaré-Friedrichs inequality in $H_0^1(\Omega)$ and is independent of mesh parameters. Also, it is clear that C_2 depends only on ω , $\|\alpha\|_{L_\infty(\Omega)}$, and C_1 .

Consider the operator $P_0 := A_0^{-1}Q_0(A+M) : \mathbf{S}_h^1 \rightarrow \mathbf{V}_0$. Then the estimate

$$\sup_{\mathbf{v}_h \in \mathbf{S}_h^1} \frac{\|(I - P_0)\mathbf{v}_h\|}{\|\mathbf{v}_h\|_A} = \sup_{\mathbf{v}_h \in \mathbf{S}_h^1} \frac{\|\mathbf{v}_h - \mathbf{v}_H\|}{\|\mathbf{v}_h\|_A} \leq C \sup_{\mathbf{v}_h \in \mathbf{S}_h^1} \frac{\|\mathbf{v}_h - \mathbf{v}_H\|}{\|\mathbf{v}_h\|_{H^1(\Omega)^2}} \leq CH^s$$

can be shown by using (3.2) and standard duality arguments, with some positive number $s \leq 1$, with $s = 1$ being attained in the case of the full regularity. Here, $\mathbf{v}_H = P_0\mathbf{v}_h$ is the coarse grid approximation in $\mathbf{V}_0 = \mathbf{S}_H^1$ to \mathbf{v}_h in \mathbf{S}_h^1 satisfying the variational equation

$$a(\mathbf{v}_H, \mathbf{w}_H) = a(\mathbf{v}_h, \mathbf{w}_H) \quad \text{for all } \mathbf{w}_H \text{ in } \mathbf{S}_H^1.$$

The result now follows immediately from [21, Theorem 1] and its proof, together with (4.4).

□

The following theorem gives a convergence rate estimate for the GMRES method applied to the system

$$(4.10) \quad B_{A+M}(A+M)u = B_{A+M}f.$$

It is an immediate consequence of Lemma 1 and [21, Theorem 2] (see also [5]).

THEOREM 1. *Assume the hypotheses of Lemma 1. Then the GMRES method converges when applied to the preconditioned system (4.10). Moreover, the estimate*

$$\|\mathbf{r}_m\|_A \leq \left(1 - CC_{\log}^{-4}(1 + C_{\log}^2)^{-2}\right)^{m/2} \|\mathbf{r}_0\|_A := \gamma(H/h)^{m/2} \|\mathbf{r}_0\|_A$$

holds for the residual $\mathbf{r}_m = B_{A+M}(\mathbf{f} - A\mathbf{u}_m)$ at the m -th iteration, where $C_{\log} := 1 + \log(H/h)$, $0 < \gamma(H/h) < 1$, and the constant C depends only on α , ν , and ω .

5. The Nonlinear Case. We shall solve the nonlinear problem (2.4) via Newton's method, which requires repeatedly solving linear systems involving the derivative of $L^{(N)}$. The action of the Frechet derivative of $L^{(N)}$ at \mathbf{u} is given by

$$\begin{aligned} (L^{(N)'(\mathbf{u})}\mathbf{w}, \mathbf{v}) &= \lim_{\delta \rightarrow 0} \frac{1}{\delta} \left((L^{(N)}(\mathbf{u} + \delta\mathbf{w}), \mathbf{v}) - (L^{(N)}\mathbf{u}, \mathbf{v}) \right) \\ &= \int_{\Omega} \lim_{\delta \rightarrow 0} \frac{1}{\delta} [\nu(|\nabla\tilde{u} + \delta\nabla\tilde{w}|)(\nabla\mathbf{u} + \delta\nabla\mathbf{w}) - \nu(|\nabla\tilde{u}|)\nabla\mathbf{u}] \cdot \nabla\mathbf{v} \, d\mathbf{x} \\ &:= \int_{\Omega} \left(\frac{\partial\Psi}{\partial\mathbf{u}} \nabla\mathbf{w} \right) \cdot \nabla\mathbf{v} \, d\mathbf{x} \end{aligned}$$

for all \mathbf{u}, \mathbf{v} , and \mathbf{w} in $H_0^1(\Omega)^{2N}$ (recall the notation (2.1) for \tilde{u}). The derivative denoted here by $\frac{\partial\Psi}{\partial\mathbf{u}} : H_0^1(\Omega)^{2N} \rightarrow (H_0^1(\Omega)^{2N})'$ has a dense $(2N)$ -by- $(2N)$ matrix representation with entries corresponding to the $2N$ coefficients in $H_0^1(\Omega)^{2N}$. For instance, the entry in the row corresponding to $\cos(j\omega t)$ and in the column corresponding to $\sin(k\omega t)$ is given by

$$(5.1) \quad \frac{\partial\Psi_j^c}{\partial\mathbf{u}_k^s} = \frac{2}{T} \int_0^T \zeta(\nabla\tilde{u}) \cos(j\omega t) \sin(k\omega t) \, dt,$$

where

$$\zeta(\mathbf{p}) := \begin{cases} \nu(|\mathbf{p}|)I + \frac{\nu'(|\mathbf{p}|)}{|\mathbf{p}|} \mathbf{p}\mathbf{p}^T & \text{for } \mathbf{p} \neq \mathbf{0}, \\ \nu(0)I & \text{for } \mathbf{p} = \mathbf{0}. \end{cases}$$

Note that $\frac{\partial\Psi}{\partial\mathbf{u}}$ and $L^{(N)'(\mathbf{u})}$ are symmetric.

The zeroth-order operator αD_N is linear, so its derivative is itself. Thus the Newton method is

$$\mathbf{u}^{k+1} = \mathbf{u}^k + \mathbf{w}^k,$$

where the update \mathbf{w}^k in $H_0^1(\Omega)^{2N}$ solves the variational problem

$$(5.2) \quad ((L^{(N)'(\mathbf{u}^k)} + \omega\alpha D_N)\mathbf{w}^k, \mathbf{v}) = (\mathbf{f} - L^{(N)}(\mathbf{u}^k) - \omega\alpha D_N\mathbf{u}^k, \mathbf{v})$$

for all \mathbf{v} in $H_0^1(\Omega)^{2N}$. The following lemma states that $L^{(N)'(\mathbf{u}^k)}$ is uniformly elliptic, so we again have a variational problem consisting of an elliptic bilinear form plus a skew-symmetric zeroth-order bilinear form, as in the linear case. This important observation means that we can take the same approach for preconditioning as in the linear case.

LEMMA 2. *Under the assumptions (1.2)-(1.3) for the continuously differentiable function ν , the Frechet derivative $L^{(N)'(\mathbf{u})} : H_0^1(\Omega)^{2N} \rightarrow (H_0^1(\Omega)^{2N})'$ is uniformly bounded and elliptic for all \mathbf{u} in $H_0^1(\Omega)^{2N}$, i.e.*

$$(L^{(N)'(\mathbf{u})}\mathbf{v}, \mathbf{v}) \geq C \|\mathbf{v}\|_{H_0^1(\Omega)^{2N}}$$

with $C > 0$ independent of \mathbf{u} and \mathbf{v} in $H_0^1(\Omega)^{2N}$.

Proof. By (5.1), we have

$$\begin{aligned} (L^{(N)'(\mathbf{u})}\mathbf{v}, \mathbf{v}) &= \int_{\Omega} \left(\frac{\partial\Psi}{\partial\mathbf{u}} \nabla\mathbf{v} \right) \cdot \nabla\mathbf{v} \, d\mathbf{x} = \int_{\Omega} \sum_{j,k=1}^N \sum_{\eta,\xi \in \{c,s\}} \left(\frac{\partial\Psi_j^\eta}{\partial\mathbf{u}_k^\xi} \nabla\mathbf{v}_k^\xi \right) \cdot \nabla\mathbf{v}_j^\eta \, d\mathbf{x} \\ &= \int_{\Omega} \frac{2}{T} \int_0^T (\zeta(\nabla\tilde{u})\nabla\tilde{v}) \cdot \nabla\tilde{v} \, dt \, d\mathbf{x} \geq C \int_{\Omega} \int_0^T |\nabla\tilde{v}|^2 \, dt \, d\mathbf{x}. \end{aligned}$$

The proof of the last inequality is based on the strong monotonicity of ν (1.3) and can be found, for instance, in [15, Lemma 2.11]. The result now follows from the Poincaré inequality in $H_0^1(\Omega)$ and basic properties of Fourier series. \square

Approximating $H_0^1(\Omega)^{2N}$ by the finite dimensional space $\mathbf{S}_h^N := \left(\text{span}\{\phi_j\}_{j=1}^{l_h}\right)^{2N}$, the variational problem (5.2) for the discrete Newton update \mathbf{w}_h^k in \mathbf{S}_h^N results in the nonsymmetric system of linear equations

$$(5.3) \quad (J^{(k)} + M)\mathbf{w}_h^k = \mathbf{f}_h - \mathbf{g}_h(\mathbf{u}_h^k) - M\mathbf{u}_h^k,$$

defined by

$$\begin{aligned} J_{ij}^{(k)} &= (L^{(N)})'(\mathbf{u}_h^k)\phi_i, \phi_j, & M_{ij} &= \omega(\alpha D_N \phi_i, \phi_j), \\ (\mathbf{f}_h)_i &= (\mathbf{f}, \phi_i), & (\mathbf{g}_h)_i &= (L^{(N)}\mathbf{u}_h^k, \phi_i), \end{aligned}$$

where $\{\phi_j\}_{j=1}^{2Nl_h}$ is the standard nodal basis for \mathbf{S}_h^N . The superscript in $J^{(k)}$ signifies the fact that the Jacobian matrix changes at each Newton iteration, depending on \mathbf{u}_h^k . By Lemma 2, the matrix $J^{(k)}$ is symmetric positive definite, so the system matrix of (5.3) is the sum of a symmetric positive definite matrix plus a skew-symmetric matrix. Therefore, the preconditioning approach used in the linear case can be used also in the nonlinear case. Thus we propose a simple block-diagonal preconditioner, with each of the $2N$ blocks preconditioning the discretized Dirichlet form

$$(5.4) \quad (\phi_h, \psi_h) \mapsto \int_{\Omega} \bar{\nu}(\mathbf{x}) \nabla \phi_h \cdot \nabla \psi_h \, d\mathbf{x},$$

for all piecewise linear ϕ_h and ψ_h in $H_0^1(\Omega)$, where we take the time-independent coefficient $\bar{\nu}$ to be the pointwise average reluctivity of the last Newton iterate over one time period, i.e.

$$\bar{\nu}(\mathbf{x}) := \frac{1}{T} \int_0^T \nu(|\nabla \tilde{u}_h^k(\mathbf{x}, t)|) \, dt$$

That is, we simply use the wire-basket domain decomposition method applied to (5.4) as the diagonal blocks in the preconditioner for $J^{(k)}$. This completes the definition of the preconditioner via (4.1) for the nonlinear case. Thus the convergence rate estimate of Theorem 1 holds also in the nonlinear case, with constants depending on the time-averaged coefficient $\bar{\nu}$.

We now make some remarks about the computational efficiency of the multiharmonic approach. Note that the matrix $J^{(k)}$ is computed at each Newton iteration, which involves the time integration (5.1) with cos and sin modes. If N is small, which is often the case in practice (see Remark 2), then this time integral can be computed quickly via Gaussian quadrature rules. However, N can be quite large in general, and accurate quadrature rules require computations with complexity on the order $O(N)$. Thus the overall complexity of assembling the matrices $J^{(k)}$ would be $O(N^3 h^{-3})$, as there are $(2N)^2$ blocks of the form (5.1). If N is actually large in practice, then this time integration should be approximated by a fast Fourier transform method, in order to reduce the cost of assembling the discrete system. Indeed, one of the greatest motivations for the multiharmonic approach (besides better parallelization) is the low computational complexity compared to time-stepping methods. However, this is beyond the scope of this paper, as we only use small values of N in our numerical experiments.

Table 6.1: Linear case with 8 subdomains ($H = 1/2$) and coarse mesh size $1/2$.

h	nodes	tets	GMRES	$\ (u^c, u^s) - (u_h^c, u_h^s)\ _{L_2(\Omega)^2}$
1/4	429	1536	4	0.1473
1/8	2585	12288	20	0.07904
1/16	18,225	98,304	26	0.02846
1/32	137,825	786,432	34	0.008086
1/64	1,074,370	6,291,456	46	0.002118

6. Numerical Results.

6.1. Numerical Results for the Linear Case. We first test the linear case with

$$\alpha \equiv \nu \equiv 1$$

and the exact solution given by

$$u(\mathbf{x}, t) = u^c(\mathbf{x}) \cos(\omega t) + u^s(\mathbf{x}) \sin(\omega t),$$

with $\omega = 1$ and

$$\begin{aligned} u^c(\mathbf{x}) &= \sin(4\pi x_1) \sin(4\pi x_2) \sin(4\pi x_3), \\ u^s(\mathbf{x}) &= \sin(2\pi x_1) \sin(2\pi x_2) \sin(2\pi x_3). \end{aligned}$$

Thus we solve only for the one harmonic ($N = 1$), namely $(u^c(\mathbf{x}), u^s(\mathbf{x}))$. This experiment demonstrates the effectiveness of the wire-basket domain decomposition preconditioner for constant coefficients and confirms the $O(h^2)$ convergence rate for the error in $L_2(\Omega)^2$. Recall that even in the linear case, a nonsymmetric linear system must be solved, and the preconditioner proposed in section (4) is being tested here.

In all experiments, $\Omega = (0, 1)^3$ is the unit cube, and $\beta = 1$ (cf. (4.1)). As discussed in [21], there is an interval of optimal values for β , which cannot be determined exactly in practice. Rather, the optimal values for β can be found only experimentally. Our tests revealed that, for the particular problem at hand, the domain decomposition preconditioner (βB in (4.1)) has a much greater effect than the coarse solver $A_0^{-1}Q_0$, to the extent that the overall preconditioner B_{A+M} is quite insensitive to changes in β . Therefore, taking $\beta = 1$ (or any other sufficiently positive number) seems to yield the best convergence.

Table 6.1 reports a test of the linear case with 8 cubic subdomains ($H = 1/2$) and fine tetrahedral meshes ranging in size from $h = 1/4$ to $h = 1/64$. We list the number of nodes and the number of tetrahedra (“tets”) in the entire mesh of Ω . We observe that the number of GMRES iterations grows polylogarithmically, in accordance with Theorem 1. The GMRES method restarts after every 20 iterations, and the stopping criterion is a relative tolerance less than 10^{-8} . The table also shows that the error of the piecewise-linear approximate solution (u_h^c, u_h^s) is of the order $O(h^2)$ with respect to the $L_2(\Omega)^2$ -norm, as the standard finite element theory predicts.

Table 6.2 reports a similar test for the linear case, but this time there are 64 cubic subdomains, with $H = 1/4$. Again we observe polylogarithmic growth in the number of GMRES iterations and order $O(h^2)$ error convergence in $L_2(\Omega)^2$.

Table 6.2: Linear case with 64 subdomains ($H = 1/4$) and coarse mesh size $1/4$.

h	nodes	tets	GMRES	$\ (u^c, u^s) - (u_h^c, u_h^s)\ _{L_2(\Omega)^2}$
1/16	18,993	98,304	28	0.03361
1/32	139,361	786,432	33	0.009321
1/64	1,077,440	6,291,456	50	0.002434

6.2. Numerical Results for the Nonlinear Case. Finally, we report two tests for the nonlinear case. For approximation in time, we take 3 harmonics (cf. Remark 2), so 6 Fourier coefficients in $H_0^1(\Omega)$ are being approximated. In space, we take 8 cubic subdomains ($H = 1/2$) and fine tetrahedral meshes of size ranging from $h = 1/8$ to $h = 1/32$. The right-hand-side is taken to be $\mathbf{f} = \mathbf{0}$, and the initial guess \mathbf{u}_h^0 is taken to be the $L_2(\Omega)$ -orthogonal projection into the piecewise linear space of

$$(g, g, g, g, g, g) \text{ in } H_0^1(\Omega)^6, \quad g = \sin(4\pi x_1) \sin(4\pi x_2) \sin(4\pi x_3).$$

Table 6.3 shows results for the nonlinearity

$$(6.1) \quad \nu(s) = 1 + s^2,$$

and Table 6.4 corresponds to the more realistic coefficient illustrated in figure (6.1), which is computed based on splines from the **B-H** curve for electromagnetic applications (see [16]). The latter test example leads to a strongly monotone and Lipschitz continuous problem whereas the former one is obviously not Lipschitz continuous. In both cases, we are testing the preconditioner as the Newton method converges to the exact solution, which is $\mathbf{0}$.

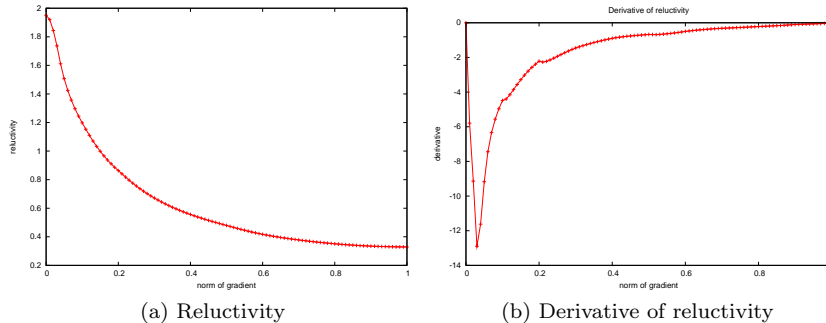


Fig. 6.1: Reactivity ν and its derivative, computed from the **B-H** curve.

The first example (6.1) does not come from a real application, but it does provide a test for the preconditioner (4.1) with a nonlinear coefficient that can become large (quadratic in the norm of the Newton iterate). Except for the coarsest test ($h = 1/8$), the Newton method converged in only 5 iterations. Since the iterations are converging to $\mathbf{0}$, the number of GMRES iterations required in each Newton step decreases. Table 6.3 reports the maximum number of GMRES iterations, which occurs in the first Newton step. The results show that the preconditioner performs well as the problem size grows.

Table 6.4 shows very fast convergence of Newton's method and the GMRES solver for each linearized step. This is due to the choice of initial guess, which is necessarily

Table 6.3: Nonlinear case, 3 harmonics, 8 subdomains ($H = 1/2$), with coarse mesh size $1/2$, ν given by (6.1).

h	nodes	tets	Newton	GMRES
1/8	2585	12288	8	≤ 131
1/16	18,225	98,304	5	≤ 32
1/32	139,361	786,432	5	≤ 20

Table 6.4: Nonlinear case, 3 harmonics, 8 subdomains ($H = 1/2$), with coarse mesh size $1/2$, ν shown in Figure 6.1.

h	nodes	tets	Newton	GMRES
1/8	2585	12288	3	≤ 14
1/16	18,225	98,304	3	≤ 15
1/32	139,361	786,432	3	≤ 14

close to the solution (zero in this case). Indeed, in this case we divided the initial guess \mathbf{u}_h^0 described above by 100, and the Newton iteration converged after only 3 iterations (the error was reduced by 6 orders of magnitude). However, the Newton iteration diverged for the initial guess $\mathbf{u}_h^0/10$. As is well known, a good initial guess is necessary for convergence of Newton's method. In practice, a good initial guess could be obtained by computing a coarse approximate solution on a hierarchy of grids.

The linear system in each numerical experiment was assembled and solved in parallel, with one subdomain per processor. This is another practical advantage of domain decomposition preconditioning, that parallel computations are easily facilitated. Moreover, the multiharmonic approach is generally more parallel than sequential time-stepping methods, since the discretization converts temporal computations (solutions at each time step) to spatial computations (more degrees of freedom for multiple Fourier coefficients). This makes multiharmonic methods more practical for large-scale computations, in addition to savings in computational complexity.

7. Conclusions. In this paper we considered an alternative time discretization method for nonlinear potential problems based on a finite approximation to the Fourier series representation of the solution. The linear system resulting from our method of numerical approximation is nonsymmetric, but consists of a symmetric positive definite matrix and a skew-symmetric matrix. We have proposed an efficient preconditioner for this linear system based on the work [21] and an inexact wire-basket domain decomposition method. The theory developed in this paper establishes a theoretical estimate of the convergence rate of GMRES as a solver when our proposed preconditioner is applied. Numerical experiments confirm this convergence rate estimate and the practical efficiency of the overall method. Of course, there are other approaches to the construction of preconditioners for the linear finite element equations (3.5). We already mentioned the preconditioner (4.5) proposed in [3]. The linear finite element equations (3.5) can be reformulated as a linear system with a symmetric but indefinite system matrix for which efficient preconditioners can be constructed based on the paper [18], see also [17] for multigrid solvers.

8. Acknowledgments. This publication is partially based on work supported by Award No. KUS-C1-016-04, made by King Abdullah University of Science and Technology (KAUST), and by the Austrian Science Fund ‘Fonds zur Förderung der wissenschaftlichen Forschung (FWF)’ under the grant P19255.

REFERENCES

- [1] F. BACHINGER, M. KALTENBACHER, AND S. REITZINGER, *An Efficient Solution Strategy for the HBE Method*, in Proceedings of the IGTE '02 Symposium Graz, Austria, 2002, pp. 385–389.
- [2] F. BACHINGER, U. LANGER, AND J. SCHÖBERL, *Numerical analysis of nonlinear multiharmonic eddy current problems*, Numer. Math., 100 (2005), pp. 593–616.
- [3] ———, *Efficient solvers for nonlinear time-periodic eddy current problems*, Comput. Vis. Sci., 9 (2006), pp. 197–207.
- [4] M. DRYJA, B.F. SMITH, AND O.B. WIDLUND, *Schwarz analysis of iterative substructuring algorithms for elliptic problems in three dimensions*, SIAM J. Numer. Anal., 31 (1994), pp. 1662–1694.
- [5] S.C. EISENSTAT, H.C. ELMAN, AND M.H. SCHULTZ, *Variational iterative methods for nonsymmetric systems of linear equations*, SIAM J. Numer. Anal., 20 (1983), pp. 345–357.
- [6] H. DE GERSEM, H. V. SANDE, AND K. HAMEYER, *Strong coupled multiharmonic finite element simulation package*, COMPEL, 20 (2001), pp. 535–546.
- [7] J. GYSELINCK, P. DULAR, C. GEUZAIN, AND W. LEGROS, *Harmonic-balance finite-element modeling of electromagnetic devices: a novel approach*, IEEE Transactions on Magnetics, 38 (2002), pp. 521–524.
- [8] G. HAASE AND U. LANGER, *The non-overlapping domain decomposition multiplicative schwarz method*, International Journal of Computer Mathematics, 44 (1992), pp. 223–242.
- [9] G. HAASE, U. LANGER, AND A. MEYER, *The approximate Dirichlet decomposition method. part I: An algebraic approach*, Computing, 47 (1991), pp. 137–151.
- [10] ———, *The approximate Dirichlet domain decomposition method. II. Applications to 2nd-order elliptic BVPs*, Computing, 47 (1991), pp. 153–167.
- [11] G. HAASE, U. LANGER, A. MEYER, AND S.V. NEPOMNYASCHIKH, *Hierarchical extension operators and local multigrid methods in domain decomposition preconditioners*, East-West J. Num. Math., 2 (1994), pp. 173–193.
- [12] G. HAASE AND S.V. NEPOMNYASCHIKH, *Extension explicit operators on hierarchical grids*, East-West J. Num. Math., 5 (1997), pp. 231–248.
- [13] M. JUNG AND U. LANGER, *Applications of multilevel methods to practical problems*, Surveys Math. Indust., 1 (1991), pp. 217–257.
- [14] G. PAOLI, O. BÍRO, AND G. BUCHGRABER, *Complex representation in nonlinear time harmonic eddy current problems*, IEEE Transactions on Magnetics, 34 (1998), pp. 2625–2628.
- [15] C. PECHSTEIN, *Multigrid-Newton-methods for nonlinear magnetostatic problems*, master’s thesis, Institute for Computational Mathematics, Johannes Kepler University Linz, 2004.
- [16] C. PECHSTEIN AND B. JÜTTLER, *Monotonicity-preserving interproximation of B-H-curves*, J. Comput. Appl. Math., 196 (2006), pp. 45–57.
- [17] J. SCHÖBERL, R. SIMON, AND W. ZULEHNER, *A robust multigrid method for an elliptic optimal control problem*, tech. report, Institute for Computational Mathematics, Johannes Kepler University Linz, 2009.
- [18] J. SCHÖBERL AND W. ZULEHNER, *Symmetric Indefinite Preconditioners for Saddle Point Problems with Applications to PDE-Constrained Optimization Problems*, SIAM J. Matrix Anal. Appl., 29 (2007), pp. 752–773.
- [19] B. SMITH, *A domain decomposition algorithm for elliptic problems in three dimensions*, Numer. Math., 60 (1991), pp. 219–234.
- [20] A. TOSELLI AND O.B. WIDLUND, *Domain decomposition methods—algorithms and theory*, vol. 34 of Springer Series in Computational Mathematics, Springer-Verlag, Berlin, 2005.
- [21] J. XU AND X.-C. CAI, *A preconditioned GMRES method for nonsymmetric or indefinite problems*, Math. Comp., 59 (1992), pp. 311–319.
- [22] S. YAMADA AND K. BESSHO, *Harmonic field calculation by the combination of finite element analysis and harmonic balance method*, IEEE Transactions on Magnetics, 24 (1988), pp. 2588–2590.
- [23] E. ZEIDLER, *Applied functional analysis*, vol. 108 of Applied Mathematical Sciences, Springer-Verlag, New York, 1995. Applications to mathematical physics.